Submitted to *Advanced Powder Technology*

Surfactant-stabilized Copper Paticles for Low-temperature Sintering: Paste Preparation using a Milling with Small Zirconia Beads: Effect of Pre-treatment with the Disperse Medium

Shuai Liu,[a.#] Rintaro Tokura,[a.#] Mai Thanh Nguyen,[a] Hiroki Tsukamoto,[a] and Tetsu Yonezawa[a,b,*]

[a]*Division of Materials Science and Engineering, Faculty of Engineering, Hokkaido University, Kita 13 Nishi 8, Kita-ku, Sapporo, Hokkaido 060-8628, Japan*

[b]*Institute for the Promotion of Business-Regional Collaboration, Hokkaido University, Kita 21 Nishi 11, Kita-ku, Sapporo, Hokkaido 001-0021, Japan*

Key Words: Copper, Fine Particle, Conductive, Paste, Milling

*Corresponding Author: Prof. Dr. Tetsu Yonezawa

Division of Materials Science and Engineering, Faculty of Engineering, Hokkaido University, Kita 13 Nishi 8, Kita-ku, Sapporo, Hokkaido 060-8628, Japan

Fax +81-11-706-7881

Abstract: Copper paste is considered as a promising candidate for printed electronics in replacement for silver paste. This is owing to copper which has anti-electromigration property, lower cost, and similar conductivity and compared with silver. We synthesize a copper nanoparticle (NP) paste that can be sintered at low temperature for high conductivity. The copper NP paste composes of 50 wt% copper NPs and dipropylene glycol (DPG) as the disperse medium. The effect of DPG coating and various conditions of milling with small beads on improving the dispersity of copper NPs has been investigated. The optimum conditions for milling are at 1000 and 2000 rpm for 30 min. This results in a volume resistivity of 6.62×10^{-6} Ω·cm after sintering the copper NP paste at 200 °C.

1. Introduction

Printed electronics has received increasing attention in the past decades owing to the simplicity and low energy consumption compared with the traditional manufacturing processes such as etching and photolithography [1-3]. Conductive patterns, layers or films can be fabricated by painting conductive paste or ink directly on desired substrates using printed electronic technology followed by sintering [4]. Examples include fabrication of integrated circuits [5], metallization for solar cells [6], and radio frequency identification tags [7] among others. Materials such as molten metals [8], conductive polymer [9], nanoparticle suspensions [10], carbon-based materials [11,12] and organometallic compounds [6,13] have been reported as conductive fillers in the conductive pastes. Among these, silver-based pastes occupy a vast portion in the conductive paste market for its high conductivity (1.6×10^{-6} Ω·cm) and resistance to oxidation in the air [14]. However, the high price and low electromigration resistance [15] of silver inhibit its large-scale application.

Copper is considered as a promising alternative for conductive component. This is because copper has low cost, similar conductivity to silver (1.7×10^{-6} Ω·cm), and an anti-electromigration property [16-21]. However, copper is susceptible to oxidation, resulting in the formation of copper oxide, which adversely affects the conductivity.

Generally, the conductive patterns are fabricated by printing the conductive pastes on blanket substrates using printed electronic technology and sintering [19]. A high sintering temperature is required for the sintering process since the melting temperature of copper is 1084 °C [21]. However, most flexible substrates are thermal sensitive that cannot withstand such a high temperature [22]. Hence, a copper paste which can be sintered at low temperature is desired. One approach to solve this issue is decreasing the size of copper particles to nano-scale to suppress the melting point, in particular surface melting, for lowering the sintering temperature. This can open the door for the use of copper paste on various substrates [23,24].

Herein, copper nanoparticles (NPs) capped by hexanoic acid were synthesized by liquid chemical reduction method using hydrazine monohydrate as the reductant. Dipropylene glycol (DPG) was used as the disperse medium for the preparation of the copper paste. Agglomerated NPs can lower the conductivity of the sintered copper paste [25]. Therefore, in this study, the effect of the pre-addition of very small amounts of DPG, *e.g.*, 5% by weight of copper, on the bead-milled redispersion of copper NPs and the optimal conditions of the bead mill to obtain a uniform copper NP paste were investigated. Finally, the copper paste was printed on alumina plate and sintered at 200 °C under a hydrogen/nitrogen (3/97, v/v) gas mixture flow. Necking among copper NPs after

sintering was examined using scanning electron microscope. The high conductivity of the sintered copper paste demonstrated its potential application for printed electronics.

2. Experimental Section

2.1 Preparation of Copper Paste

CuO micropowders (Nisshin Chemco, average particle size:1 μm) were used as copper source in this study. Dipropylene glycol (Wako, Japan), hydrazine monohydrate ($N_2H_4 \cdot H_2O$) (Wako), hexanoic acid (Junsei, Japan), acetone (Kanto, Japan), methanol (Wako) and ethanol were used as received without any purification. Deionized (DI) water was prepared using ELGA/Organo Purelabo system (> 18 MΩ).

Firstly, copper nanoparticles were synthesized by chemical reduction method using hydrazine as the reducing reagent, which is similar to the previous process. [26] With the obtained nanoparticles, copper paste was prepared with dipropylene glycol as the disperse medium. 79.5g (1 mol) of CuO micropowder was dispersed in 1 L of ethanol with a stirring speed of 250 rpm. Hexanoic acid (60 mmol, 7.5 mL) as the stabilizer was added to the dispersion. After that, the dispersion was heated up to 70 °C by water bath. Hydrazine (2.0 mol, 97 mL) acting as reducing agent was then added to the dispersion. The dispersion was kept at 70 C for 1h. The reaction was terminated by cooling the

mixture to room temperature. Prepared copper nanoparticles were then collected by centrifugation (400 G) and washed by acetone twice and methanol twice. Small amount (5 wt%) of dipropylene glycol (DPG) was added to the collected copper nanoparticles. Then, the particles were dried under nitrogen atmosphere at room temperature overnight. The dried copper powder was ground for 30 min using a mortar and crushed for 5 min using a mixing blender in order to reduce agglomeration of the particles according to the results from previous study as described. [27] Then, the paste of copper nanoparticles (50 wt%) in DPG was prepared using a hybrid mixer (4 min × 3). The obtained copper paste was milled with a bead-mill with zirconia beads (30 μm) with designated conditions. For comparison, a paste of copper fine nanoparticles (50 wt%) was also prepared without pre-addition of DPG. After the preparation, metal mesh filter (1 μm) was applied in order to eliminate big agglomerates.

2.2 Printing of the Copper Pastes and Sintering

The obtained copper pastes were printed on an alumina substrate using a doctor blade with a thickness of 40 μm. The blade was moved from one side of the plate to the other to form a smooth film on the alumina substrate under ambient conditions. Sintering was carried out in a tube furnace.

2.3.Characterizations

The particle sizes were determined using a field emission scanning electron microscope (FE-SEM; JEOL JSM-6701F) and transmission electron microscope (TEM; JEM-2000FX, 200 kV). The morphologies of surfaces and cross-sections the copper layers before and after sintering were observed also using FE-SEM. The crystalline structures of the samples were analysed by X-ray diffractometer (XRD; Rigaku Miniflex II) at 2θ from 20° to 80°.

Thermogravimetric/differential thermal analysis (TG/DTA; Shimadzu DTA-60H) was carried out to evaluate thermal decomposition behaviour of the prepared copper paste. The sample was subjected to a flow rate of 100 mL·min^{-1} 3%H_2/N_2 gas or N_2 gas at a temperature ranging from 20 °C to 500 °C with a heating rate of 5 °C min^{-1}.

Resistance of the sintered copper layers were carried out by a four-point-probe measurement with a Loresta-GP (Mitsubishi Chemical). Moreover, the thickness of the copper layer was determined by examination of its cross-sectional SEM images.

3. Results and Discussions

3.1. Particle size and crystal structure of the prepared copper NPs

The mean size of copper NPs was obtained by measuring 200 NPs in the SEM and TEM image (Figure 1(a)). The average diameter of copper NPs is 82 ± 18 nm from SEM and 74 ± 28 nm from TEM image. The difference is caused by the fact that small copper NPs were found more readily in the TEM image compared with those in the SEM image. It is probably due to the difference of the resolutions and the coating of organic layer which can be clearly observed only in the SEM image. Figure 2 shows the XRD pattern of the synthesized metallic copper sample. All peaks are in good agreement with the simulated Cu reference pattern. There are possibly some very weak and broad signal from Cu_2O around $2\theta = 36$ °, that indicates that the particle surface is slightly oxidized.

3.2. Effect of pre-addition of DPG before milling

A set of comparative experiments was conducted to study the effect of pre-addition of the solvent of the copper paste, that is, DPG. Figure 3 shows the SEM images of copper NPs with and without pre-addition of DPG. Both samples were ground for 30 min by a mortar and crushed for 5 min using a mixing blender then made into copper paste before SEM observation. It is observed that the number of the agglomerations of particles considerably decreased as DPG was pre-added before crushing. The size of the agglomerates of copper NPs decreased from about 10 μm to 2 μm when DPG was pre-added. This demonstrates

that pre-addition of DPG to copper NPs before dispersing played important role in dispersing copper NPs. The hexanoic acid-stabilized copper nanoparticles are hydrophobic due to the hexanoic acid layer with the alkyl chain outside on the particle surface. Therefore, the pre-coating with DPG just after the preparation could improve the dispensability of these hydrophobic nanoparticles into the same medium.

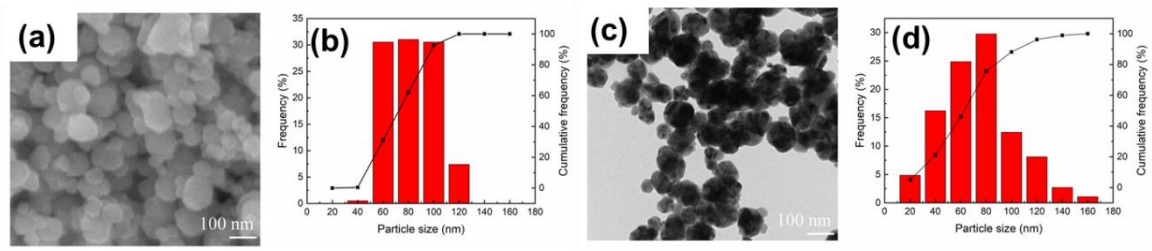

Fig. 1. (a) SEM and (b) TEM images of the obtained copper nanoparticles. (b, d) the size distributions obtained from TEM and SEM images, respectively.

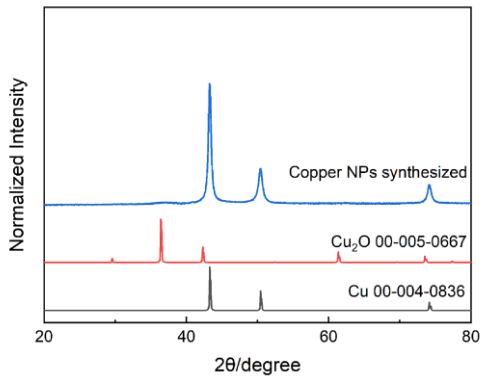

Fig. 2. X-ray diffraction pattern of the obtained copper nanoparticles. The reference patterns are $Cu_{64}O$, Cu_2O and metallic Cu.

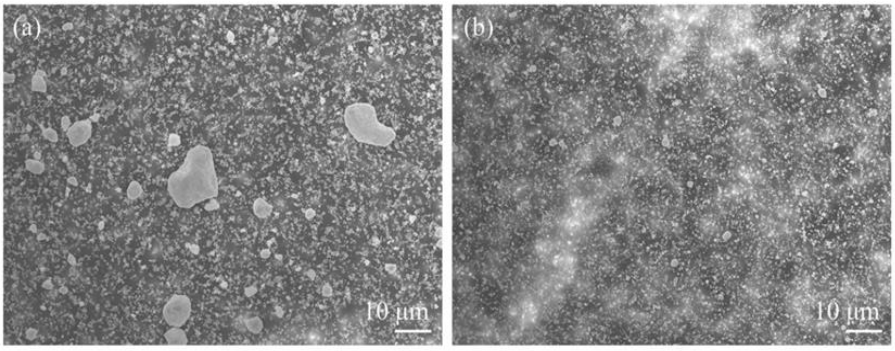

Fig. 3. SEM images of the printed copper samples (a) without and (b) with pre-addition of DPG.

The copper paste after mixing copper NPs and DPG was milled with small beads at 1000, 2000, 2500 rpm continuously under nitrogen atmosphere for 30 min. Figure 4 shows the SEM images of the samples after milling. Many loose agglomerations were observed after milling at 1000 rpm for 30 min. Large fused particles (arrows in Figures 4e and 4f) appeared after continuously milled at 1000, 2000, and 2500 rpm. Figures 4c and 4d show that copper NPs were dispersed independently. Therefore, we have selected that the milling at 1000 and 2000 rpm (30 min each) was the optimum conditions for milling with the zirconia beads.

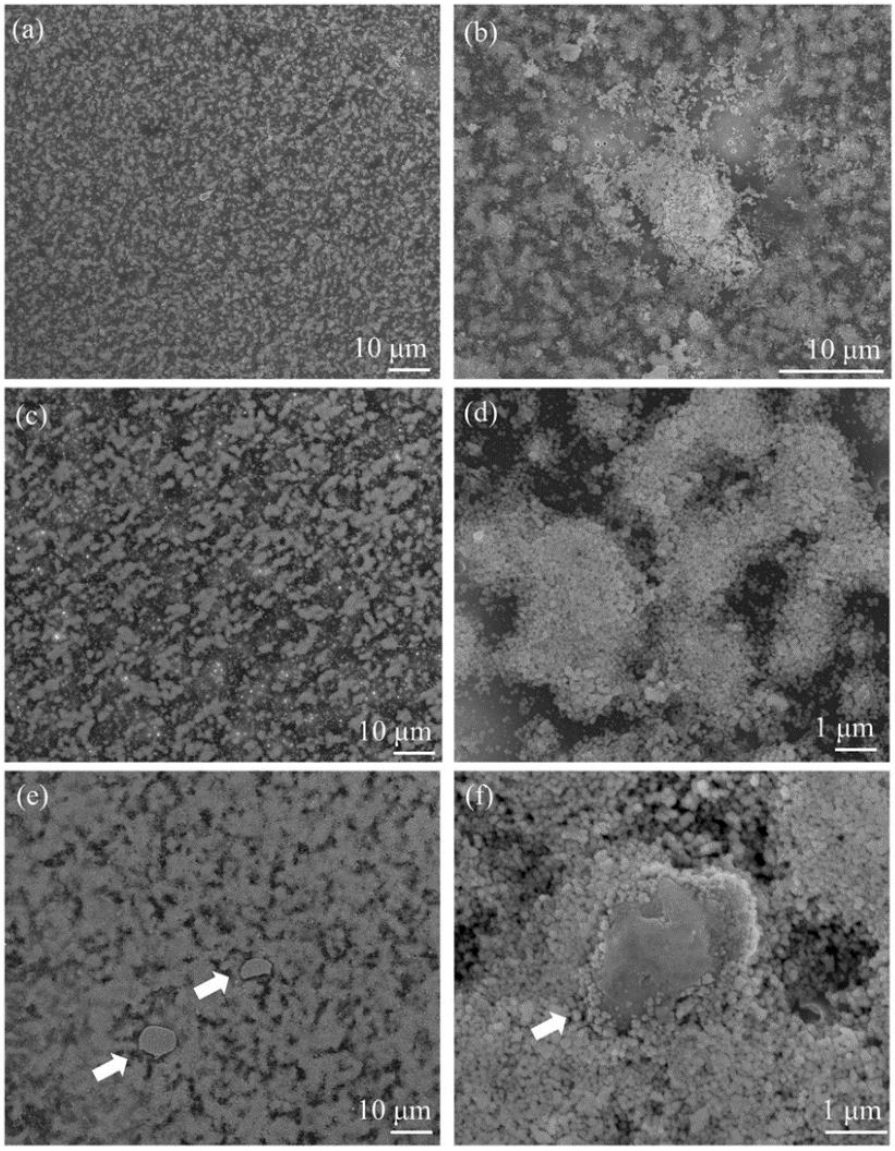

Fig. 4. SEM images of the copper paste milled at (a, b) 1000 rpm, (c, d) 1000 + 2000 rpm, (e, f) 1000 + 2000 + 2500 rpm continuously. Each milling time was 30 min. Arrows in (e) and (f) indicates the fused particles. Pre-addition of DPG was applied for the copper NPs.

We have also prepared a copper paste with copper NPs without DPG-pre-addition. Unfortunately, the obtained paste could not pass the metal mesh filter (1 mm)

according to the large agglomerates as observed in Figure 3(a). X-ray diffraction patterns of the obtained pastes of copper NPs with and without pre-addition of DPG are collected in Fig. 5. The XRD patterns of the copper pastes obtained from copper NPs with and without DPG pre-addition are almost identical.

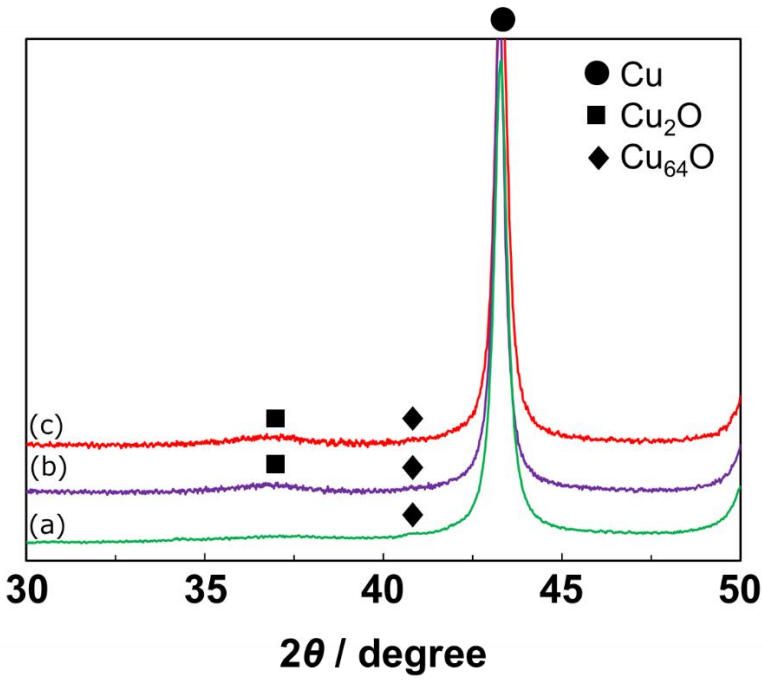

Fig. 5. X-ray diffraction patterns of (a) as prepared copper NP powder, (b) the copper paste of the copper NPs with pre-addition of DPG, and (c) the copper paste of the copper NPs without pre-addition of DPG.

The oxide content of the copper nanoparticles obtained by crystalline phase analysis with the RIR method from the x-ray diffraction patterns in Figures 5b and 5c is

summarized in Table 1. From these results, we can conclude that pre-addition of DPG do not affect the oxidation of copper NPs during the preparation of copper pastes.

Table 1. Crystalline phase analysis by x-ray diffraction patterns[a] of copper NPs in the copper pastes prepared with and without pre-addition of DPG by using reference intensity ratio (RIR) method

Sample	$Cu_{64}O$	Cu_2O	Cu
Copper NPs without pre-addition of DPG	0.9	4.1	94.9
Copper NPs with pre-addition of DPG	0.8	4.9	94.3

[a]Diffraction patterns used for the analyses are shown in Fig. 5.

3.3. Thermogravimetory-differential thermal analyses (TG-DTA) of the obtained copper nanoparticles

In order to determine sintering temperature, TG-DTA was carried out for the copper paste under H_2/N_2 (3/97 v/v) gas mixture flow and the result is shown in Figure 5. The mass loss found in the temperature range of 100 – 180 °C can be attributed to the evaporation of DPG. No obvious weight loss or increase can be observed in the higher temperature range. The obtained DTA curve also revealed one endothermic peak in the same range,

which also suggested the evaporation of DPG. Judging from this result, we decided to sinter our particles at 200 °C. The small exothermic peak found around 235 °C is corresponding to the reduction of copper oxide to copper. The peak found in the TG-DTA curve of this sample observed under nitrogen gas flow (Fig. 6(b)) was considerably smaller than the peak found in Fig. 6(a) which was taken under reductive 3 % hydrogen-nitrogen gas flow.

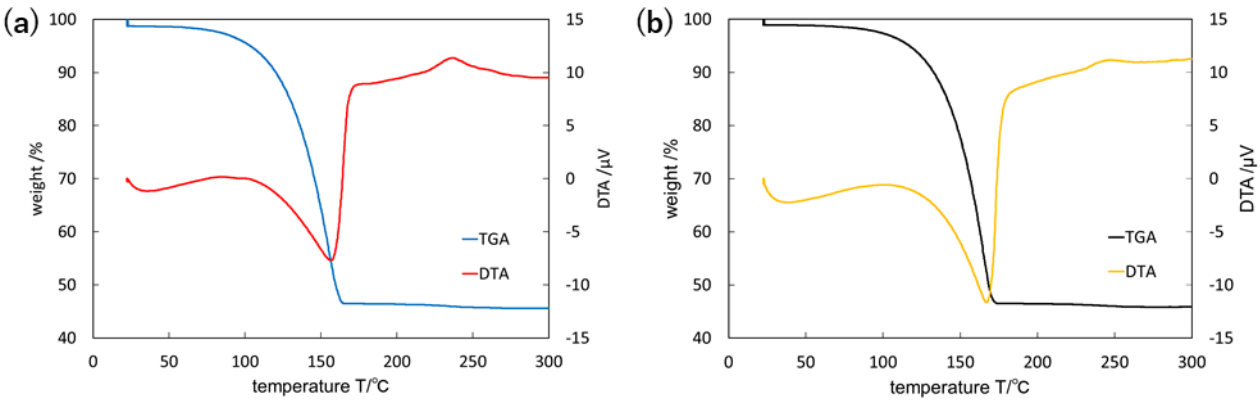

Fig. 6. TG-DTA curves of the copper paste (~ 25 mg) in DPG. The measurement was carried out under (a) 3%H_2-N_2 gas flow and (b) N_2 gas flow.

3.4. Sintering of the obtained copper paste on an alumina substrate

The printed layers of the copper NPs were sintered at 200 °C in the tube furnace for 1 h under H2/N2 (3/97, v/v) gas mixture flow. Figure 6 shows the surface and cross-sectional SEM images of the copper layer after sintering. The flat surface of the printed layers as

shown in Fig. 7(b) indicates great dispersity of the copper NPs in the paste. Large neckings and particle networks can be clearly observed in the magnified image (Fig. 7(c)) which suggests a high conductivity of this copper layer. Compact copper nanoparticles layers and tight connections among copper nanoparticles observed contributed to the high conductivity of the copper layer. The thickness of the obtained copper layer measured using cross-sectional SEM image (Fig. 7(a)) was 2.72 ± 0.49 μm. By a four-point probe measurement, the surface resistivity of the layer was 0.02435 Ω□ and the resistivity could be calculated as 6.62×10^{-6} Ω·cm, which is about 4 times of the bulk copper (1.68×10^{-6} Ω·cm).

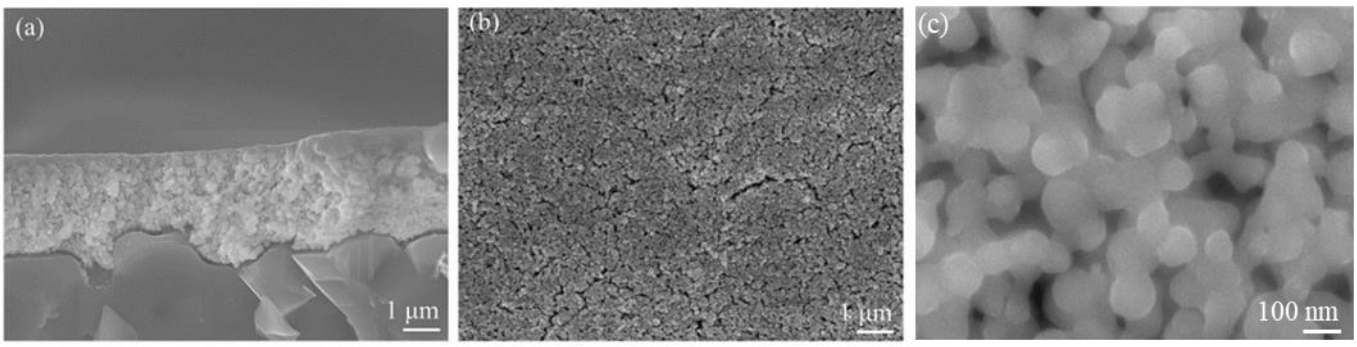

Fig. 7. SEM images of (a) Cross-sectional and (b, c) surface of the copper layer sintered at 200 °C.

Conclusion

In summary, a copper NP paste comprising copper NPs (50 wt%) and dipropylene glycol (DPG) was prepared in this study for low-temperature sintering. The size of agglomerates of copper NPs decreased with pre-addition of DPG. Further, size agglomerations were eliminated by milling with small zirconia beads at the optimum rotation rate of 1000 and 2000 rpm for 30 min each for preparing the copper paste. The resistivity of the copper paste sintered at 200 °C was 6.62×10^{-6} Ω·cm. DPG pre-addition did not affect the oxidation state of copper NPs. This study demonstrates an effective method based on pre-addition of DPG and beads milling to eliminate agglomerates of hexanoic acid-coated copper nanoparticles for production of copper paste which can be sintered for a high conductivity.

Acknowledgements:

This work is partially supported by Hokkaido University and Grant-in-Aid for Challenging Research (Exploratory) (19K22094 to TY) and Fund for the Promotion of Joint International Research (Fostering Joint International Research (B)) (18KK0159 to TY and MTN) from JSPS, Japan. A3 Foresight Program "Organic/Inorganic Nanohybrid Platforms for Precision Tumor Imaging and Therapy" from JSPS is also gratefully acknowledged. It was also partially supported by the Management Expenses Grants for

Network Joint Research Center for Materials and Devices (20201248 and 20191253). Authors thank Drs. Y. Ishida (Hokkaido Univ.), T. Sugahara (Osaka Univ.) and T. Tokunaga (Nagoya Univ.) for fruitful discussions.

Note and References:

[#]Equal contribution for the first two authors.

[1] A. Yabuki and S. Tanaka, Electrically conductive copper film prepared at low temperature by thermal decomposition of copper amine complexes with various amines, Mater. Res. Bull. 47 (2012) 4107-4111.

[2] H. H. Lee, K. S. Chou and K. C. Huang, Inkjet printing of nanosized silver colloids, Nanotechnology 16 (2005) 2439-2441.

[3] A. C. Arias, J. D. MacKenzie, I. McCulloch, J. Rivnay, and A. Salleo, Materials and Applications for Large Area Electronics: Solution-Based Approaches, Chem. Rev. 110 (2010) 3-24.

[4] C. H. Lee and J.-H. Lee, Characterization of Copper Complex Paste: Manufacture of Thin Cu-Seed Films on Alumina Substrates, Elec. Mater. Lett. 15 (2019) 247-252.

[5] H. Sirringhaus, T. Kawase and R. Friend, High-Resolution Ink-Jet Printing of All-Polymer Transistor Circuits, MRS Bull. 26 (2001) 539-543.

[6] S. H. Lee, D. W. Lee and S. H. Lee, Review of Conductive Copper Paste for c-Si Solar Cells, Korean J. Metals Mater. 55 (2017) 637-644.

[7] V. Sanchez-Romaguerra, S. Wünscher, B. M. Turki, R. Abbel, S. Barbosa D. J. Tate, D. Oyeka, J. C. Batchelor, E. A. Parker, U. S. Schubert S. G. Yeates, J. Mater. Chem. C 3 (2015) 2132.

[8] Q. Liu and M. Orme, High precision solder droplet printing technology and the state-of-the-art, J. Mater. Proc. Tech. 115 (2001) 271-283.

[9] C.-W. Lee, D.-H. Nam, Y.-S. Han, K.-C. Chung and M.-S. Gong, Humidity sensors fabricated with polyelectrolyte membrane using an ink-jet printing technique and their electrical properties, Sens. Actuators B 109 (2005) 334-340.

[10] P. Calvert, Inkjet Printing for Materials and Devices, Chem. Mater. 13 (2001) 3299-3305.

[11] M. Lin, Y. Gai, D. Xiao, H. Tan, and Y. Zhao, Preparation of pristine graphene paste for screen printing patterns with high conductivity, Chem. Phys. Lett. 713 (2018) 98-104.

[12] J. Wang, H. Tan, D. Xiao, R. Navik, M. Goto and Y. Zhao, Preparation of waterborne graphene paste with high electrical conductivity, Chem. Phys. Lett. 741 (2020) 137098.

[13] K. Wang, M. D. Paine, and J. P. W. Stark, Fully voltage-controlled electrohydrodynamic jet printing of conductive silver tracks with a sub-100 μm linewidth, J. Appl. Phys. 106 (2009) 024907.

[14] Y. Jo, S.-J. Oh, S. S. Lee, Y.-H. Seo, B.-H. Ryu, J. Moon, Y. Choi, S. Jeong, Extremely flexible, printable Ag conductive features on PET and paper substrates via continuous millisecond photonic sintering in a large area, J. Mater. Chem. C, 2 (2014) 9746-9753.

[15] G. Ripka and G. Harsanyi, ELECTROCHEMICAL MIGRATION IN THICK-FILM IC-S, Electrocomp. Sci. Tech., 11 (1985) 281-290.

[16] K. Ida, M. Tomonari, Y. Sugiyama, Y. Chujyo, T. Tokunaga, T. Yonezawa, K. Kuroda, K. Sasaki, Behavior of Cu nanoparticles ink under reductive calcination for fabrication of Cu conductive film, Thin Solid Films, 520 (2012) 2789-2793.

[17] Y. Y. Dai, M. Z. Ng, P. Anatha, Y. D. Lin, Z. G. Li, C. L. Gan, C. S. Tan, Enhanced copper micro/nano-particle mixed paste sintered at low temperature for 3D interconnects, Appl. Phys. Lett., 108 (2016) 263103.

[18] W. Guo, H. Zhong, X. Zhang, L. Liu, P. Peng, G. Zou, Y. N. Zhou Preparation of nanoparticle and nanowire mixed pastes and their low temperature sintering, J. Alloys Compounds, 690 (2017) 86-94.

[19] H. Min, B. Lee, S. Jeong, M. Lee, Laser-direct process of Cu nano-ink to coat highly

conductive and adhesive metallization patterns on plastic substrate, Opt. Lasers Eng., 80 (2016) 12-16.

[20] T. Yonezawa, H. Tsukamoto, M. T. Nguyen, Particle size tuning in scalable synthesis of anti-oxidized copper fine particles by polypeptide molecular weights, Adv. Powder Tech., 28 (2017) 1966-1971.

[21] T. Yonezawa, S. Takeoka, H. Kishi, K. Ida and M. Tomonari, The preparation of copper fine particle paste and its application as the inner electrode material of a multilayered ceramic capacitor, Nanotechnology 19 (2008) 145706.

[22] W.-Y. Chung, Y.-C. Lai, T. Yonezawa, Y.-C. Liao, Nanomaterials, Sintering Copper Nanoparticles with Photonic Additive for Printed Conductive Patterns by Intense Pulsed Light, 9 (2019) 1071.

[23] Y. Yong, M. T. Nguyen, H. Tsukamoto, M. Matsubara, Y.-C. Liao, T. Yonezawa, Effect of decomposition and organic residues on resistivity of copper films fabricated via low-temperature sintering of complex particle mixed dispersions, Sci. Rep., 7 (2017) 45150.

[24] A. Yabuki and N. Arriffin, Electrical conductivity of copper nanoparticle thin films annealed at low temperature, Thin Solid Films, 518 (2010) 7033-7037.

[25] W.-C. Chang, L.-W. Weng, C.-K. Chuang, J.-X. Liang, T.-N. Yang, W.-Y. Ma, The

Preparation of Antioxidant Copper Paste and Its Application to Silicon Solar Cells, J. Nanosci. Nanotechnol. 16 (2016) 9125-9131.

[26] T. Yonezawa, J. Shi, H. Tsukamoto, M. T. Nguyen, Size-controlled Preparation of Alkylamine-stabilized Copper Fine Particles from Cupric Oxide (CuO) Micro-particles, MRS Adv., 4 (2019) 413-418.

[27] Y. Yong, T. Yonezawa, M. Matsubara, H. Tsukamoto, The mechanism of alkylamine-stabilized copper fine particles towards improving the electrical conductivity of copper films at low sintering temperature, J. Mater. Chem. C, 3 (2015) 5890-5895.